BIOCHEMISTRY
including biophysical chemistry & molecular biology
Article

Biochemistry **2010,** *49,* 2121–2129 2121
DOI: 10.1021/bi901829f

Insights into the Conformational Dynamics of the E3 Ubiquitin Ligase CHIP in Complex with Chaperones and E2 Enzymes[†]

Christian Graf,[‡] Marta Stankiewicz, Rainer Nikolay, and Matthias P. Mayer*

Zentrum für Molekulare Biologie der Universität Heidelberg, DKFZ-ZMBH Alliance, Heidelberg, Germany.
[‡]Current address: Novartis Biologics, Novartis Pharma AG, 4002 Basel, Switzerland.

Received October 26, 2009; Revised Manuscript Received February 9, 2010

ABSTRACT: The dimeric E3 ubiquitin ligase CHIP binds with its tetratricopeptide repeat (TPR) domain the C-terminus of molecular chaperones Hsp70 and Hsp90 and with its U-box region E2 ubiquitin-conjugating enzymes. By ubiquitinating chaperone-bound polypeptides, CHIP thus links the chaperone machinery to the proteasomal degradation pathway. The molecular mechanism of how CHIP discriminates between folding and destruction of chaperone substrates is not yet understood. Two recently published crystal structures of mouse and zebrafish CHIP truncation constructs differ substantially, showing either an asymmetric assembly or a symmetric assembly with a highly ordered middle domain. To characterize the conformational properties of the intact full-length protein in solution, we performed amide hydrogen exchange mass spectrometry (HX-MS) with human CHIP. In addition, we monitored conformational changes in CHIP upon binding of Hsp70, Hsp90, and their respective C-terminal EEVD peptides, and in complex with the different E2 ubiquitin-conjugating enzymes UbcH5a and Ubc13. Solution HX-MS data suggest a symmetric dimer assembly with highly flexible parts in the middle domain contrasting both the asymmetric and the symmetric crystal structure. CHIP exhibited an extraordinary flexibility with a largely unprotected N-terminal TPR domain. Formation of a complex with intact Hsp70 and Hsp90 or their respective C-terminal octapeptides induced folding of the TPR domain to a defined, highly stabilized structure with protected amide hydrogens. Interaction of CHIP with two different E2 ubiquitin-conjugating enzymes, UbcH5a and Ubc13, had distinct effects on the conformational dynamics of CHIP, suggesting different roles of the CHIP−E2 interaction in the ubiquitination of substrates and interaction with chaperones.

The C-terminus of Hsc70 interacting protein (CHIP)[1] is a cochaperone that links Hsc70/Hsp70 and Hsp90 chaperones to the ubiquitin proteasomal degradation pathway as a function complementary to protein stabilization and refolding in protein quality control (*1*). It was proposed that CHIP takes part in the protein triage decision distinguishing chaperone clients that could be salvaged and hopeless cases (*2*).

CHIP is a dimeric 35 kDa multidomain protein composed of an N-terminal tetratricopeptide repeat (TPR) domain, a middle domain responsible for dimerization, which was shown to be important for CHIP's function in ubiquitination (*3*), and a U-box domain that is structurally related to RING finger type E3 ligase involved in the ubiquitination cascade (*4*) (Figure 1a). Unlike the HECT domain E3 ligases, which transiently bind ubiquitin covalently during the transfer onto the substrate, E3 enzymes containing a RING domain (zinc finger really interesting new gene) enable the direct transfer of ubiquitin from the E2 ubiquitin-conjugating enzyme to the substrate lysine side chain, serving as a scaffold. Two different E2 enzymes have been shown to interact with the U-box of CHIP, members of the UbcH5 family, which can form canonical Lys^{48}−ubiquitin chains but also other linkages, and the noncanonical Lys^{63}-specific ubiquitin-conjugating enzyme Ubc13−Uev1a complex (*5*, *6*). Structural information about this interaction is available for hCHIP U-box constructs in complex with the Ubc13−Uev1 structure (*6*) and the CHIP−U-box−UbcH5 complex from *Danio rerio* (*7*), revealing electrostatic and hydrophobic interaction between CHIP's U-box and a Ser-Pro-Ala binding motif, which is conserved in all E2-conjugating enzymes.

The N-terminal TPR domain of CHIP consists of seven helices in helix−turn−helix arrangements that were shown to specifically interact with the C-terminal EEVD motif of molecular chaperones Hsp70 and Hsp90. Full-length mouse CHIP (residues 23−303) was crystallized in complex with a peptide comprising the C-terminus of Hsp90 (DDTSRMEEVD) and revealed a dimeric assembly with an asymmetric arrangement: in one protomer, helix α7 of the TPR domain is elongated continuing into the helix−turn−helix motif of the middle domain, while in the other protomer, the helical hairpin of the middle domain is connected to the TPR domain via an unfolded region (*6*) (Figures 1b and 2). In contrast to the TPR domains of adaptor protein Hop/Sti1, which discriminate between the C-termini of Hsp70 and Hsp90, the TPR domain of CHIP binds the C-termini of both chaperones promiscuously. The crystal structure of the CHIP−peptide complex revealed that the peptide is bound in a curled conformation in which only the common (M/I)EEVD

[†]This work was supported by the Deutsche Forschungsgemeinschaft (SFB638 A13).

*To whom correspondence should be addressed: Im Neuenheimer Feld 282, 69120 Heidelberg, Germany. Telephone: +49 (0)6221 546829. Fax: +49 (0)6221 545894. E-mail: M.Mayer@zmbh.uni-heidelberg.de.

[1]Abbreviations: CHIP, C-terminus of Hsc70 interacting protein; HX, amide hydrogen $^{1}H-^{2}H$ exchange; MS, mass spectrometry; TPR, tetratricopeptide repeat; SPR, surface plasmon resonance spectroscopy; PDB, Protein Data Bank.

Published on Web 02/10/2010

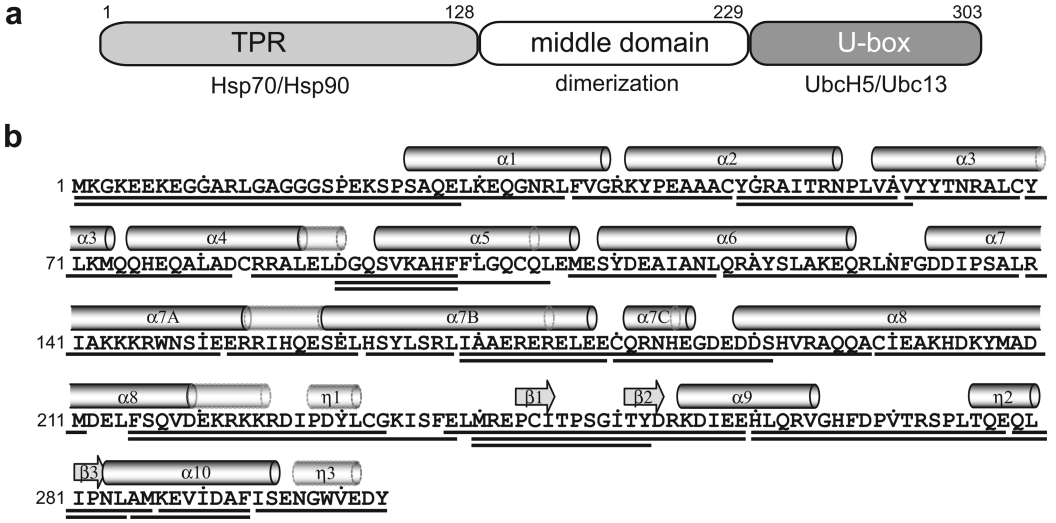

FIGURE 1: Domain structure and sequence of human CHIP. (a) Domain architecture of hCHIP. The TPR domain binds to the EEVD motif of Hsp70 and Hsp90 chaperones. The middle domain constitutes a helical hairpin that is responsible for dimerization. The C-terminal U-box domain interacts with E2 ubiquitin-conjugating enzymes. (b) Amino acid sequence of hCHIP and sequence coverage of peptic peptides analyzed in the HX-MS experiment. Each assigned peptide is denoted with a black bar underneath the sequence. Secondary structure elements on top are derived from the crystal structure of mouse CHIP (PDB entry 2C2L). Transparent cylinders with dashed lines indicate the differences between the two conformations of the asymmetric assembly.

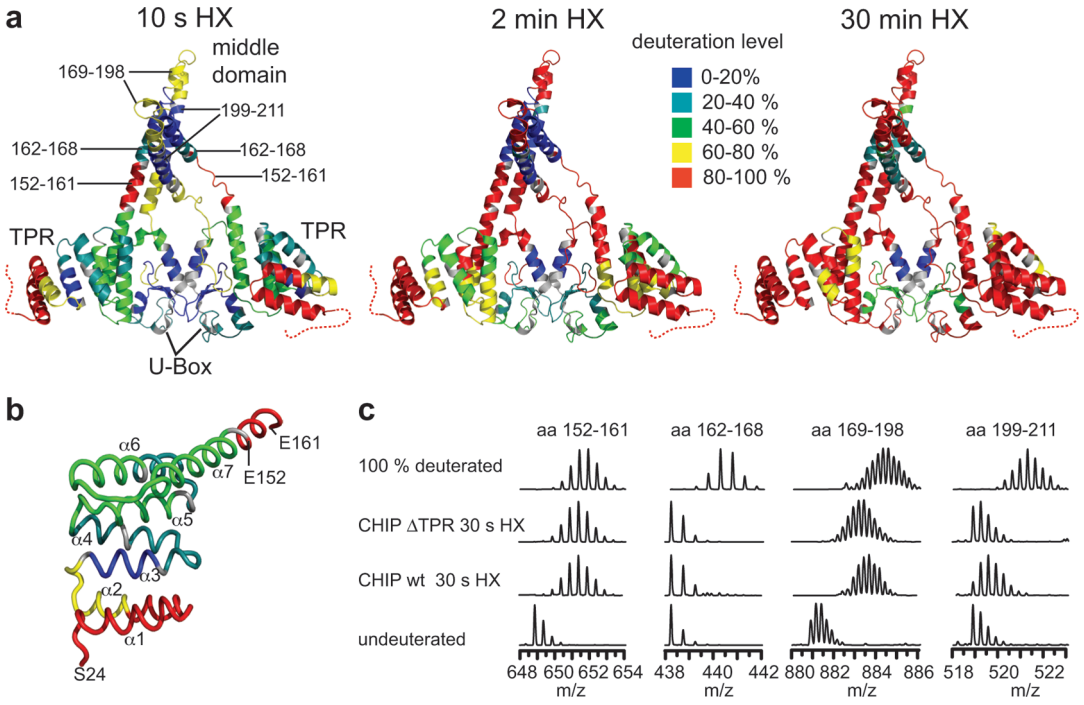

FIGURE 2: Conformational flexibility of CHIP. (a) Time-dependent deuteron incorporation shown in a cartoon representation of the asymmetric mouse CHIP dimer structure in complex with MEEVD peptides (residues 25−304, PDB entry 2C2L). The deuteration level of analyzed peptides after 10 s, 2 min, and 30 min in D_2O is shown with a color code. Gray color indicates regions for which no exchange data are available. The dashed line symbolizes the 24 N-terminal residues missing in the crystal structure. (b) Deuteron incorporation in apo-CHIP segments in the TPR domain after 10 s in D_2O. The first and last residues are indicated. (c) Original spectra of CHIP peptic peptide amino acids 152−161, 162−168, 169−198, and 199−211 (representing segments 153−161, 163−168, 170−198, and 200−211, respectively, in Figure 3; see footnote [2]) in the undeuterated, 30 s deuterated, and fully deuterated states. For the sake of comparison, the experiment was performed with wild-type hCHIP and hCHIP(128−303) lacking the TPR domain.

sequence is in contact with the TPR domain, allowing binding of different types of chaperones. A recent crystal structure of zebrafish CHIP lacking the TPR domain differs substantially from the mouse CHIP structure, showing a symmetric dimer assembly with elongated helices in the middle domains of both protomers (*8*). Interestingly, the overlay of the 2:2:2 complex of the U-box of CHIP with Ubc13 and Uev1 with the crystal structure of full-length mouse CHIP shows that only one of the two Ubc13−Uev1 dimers fits in the structure while the other would induce sterical clashes with one of the TPR domains of the CHIP dimer (*6*). Isothermal titration calorimetry experiments supported the asymmetric 2:1:1 complex of full-length CHIP with Ubc13 and Uev1 (*6*). Similarly, UbcH5a, which binds to the U-box of CHIP in a manner almost identical to that of Ubc13,

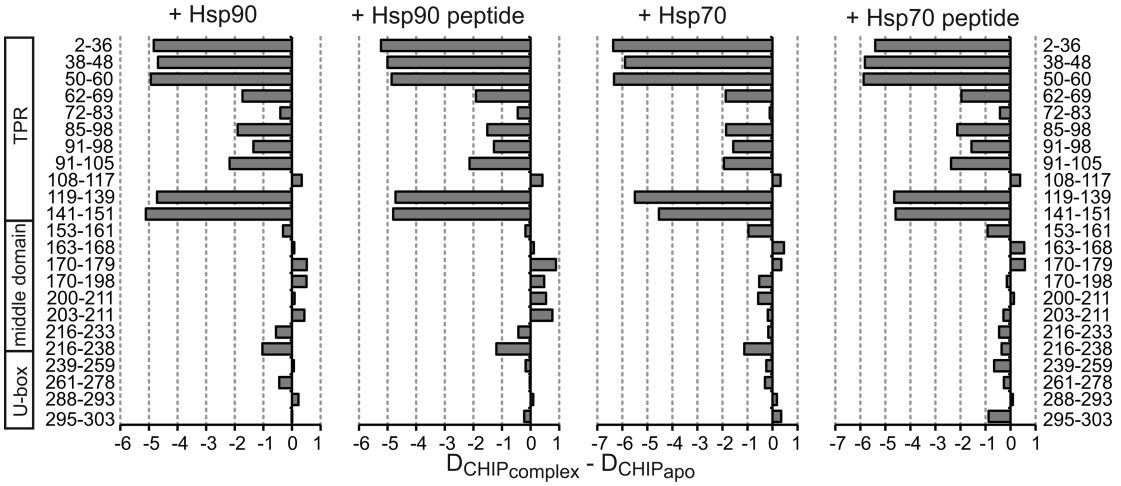

FIGURE 3: Effects of TPR−ligand binding on the incorporation of deuterons into CHIP segments. Shown are the differences between the number of deuterons incorporated into CHIP segments when CHIP is in complex with human Hsp90, Hsp70, or octapeptides ASRMEEVD (Hsp90 C-terminus) and GPTIEEVD (Hsp70 C-terminus) and the number of deuterons incorporated in the absence of ligand after 30 s in D_2O. Negative values thus indicate stabilization and protection of amide hydrogens from solvent in the presence of the respective ligand.

should also bind to full-length CHIP in an asymmetric 2:1 complex. Thereby, the symmetric Hsp90 chaperone dimer would be linked through the asymmetric CHIP to an unpaired ubiquitin-conjugating enzyme. Despite this wealth of structural data, it remains unclear how the CHIP homodimers of two identical subunits become the functional asymmetric protein.

In this study, we investigated the conformational properties of intact human CHIP in solution using amide hydrogen $^1H-^2H$ exchange (HX) combined with mass spectrometry (MS). By determining the solvent accessibility of backbone amide hydrogens, this technique allows the analysis of the stability and dynamics of protein secondary structure and protein motions related to protein−protein interactions, protein−ligand interactions, and allostery (*9*−*11*). We observed major conformational changes upon binding of full-length Hsp70 and Hsp90 chaperones or their respective C-terminal EEVD-containing peptides, and in complex with the E2 ubiquitin-conjugating enzymes UbcH5a and Ubc13 that provide insights into the structural dynamics of CHIP in the cell.

EXPERIMENTAL PROCEDURES

Peptides and Protein Expression and Purification. Synthetic peptides ASRMEEVD (Hsp90 peptide) and GPTIEEVD (Hsp70 peptide) were purchased from Thermo Fisher Inc. Human CHIP and CHIPΔTPR(128−303) were expressed in *Escherichia coli* and purified as described previously (*3*). Human Hsp90β, Hsc70, Hsp70, and Ubc13 were cloned into bacterial expression vector pCA528 encoding an N-terminal His_6-Smt3 tag (*12*). The fusion proteins were overexpressed in *E. coli* strain BL21(DE3)Star/pCodonPlus (Invitrogen). The cultures were grown to an OD_{600} of 0.6, and expression was induced with 0.5 mM IPTG for 5 h at 30 °C. Cells were lysed by a microfluidizer (Avestin EmulsiFlex-C5) in lysis buffer A [20 mM HEPES-KOH (pH 7.6), 100 mM KCl, 5 mM $MgCl_2$, 5% glycerol, and 1 mM β-mercaptoethanol] and 5 mM PMSF, 1 mM pepstatin A, 1 mM leupeptin, and 1 mM aprotinin. The lysate was clarified by centrifugation (40000 rpm for 30 min) and incubated with Ni^{2+}-IDA matrix (Protino, Macherey-Nagel) for 30 min. After incubation, the matrix was washed with buffer A and bound protein eluted with buffer A containing 250 mM imidazole. The eluted fusion proteins were supplemented with Ulp1 protease, which cleaved the His_6-Smt3 tag, and the mixture was dialyzed overnight against buffer A containing 10 mM KCl. Cleaved recombinant proteins were recovered in the flow-through fractions after a second incubation with Ni^{2+}-IDA matrix, whereas the N-terminal His_6-Smt3 tag and Ulp1 remained on the column. Proteins were further purified by anion exchange chromatography (ReSourceQ, GE Healthcare) with a linear gradient from 0.01 to 1 M KCl, followed by Superdex 200 size exclusion chromatography in buffer B [20 mM HEPES (pH 7.6), 300 mM KCl, 5% glycerol, and 1 mM DTT], and finally dialyzed against storage buffer [20 mM HEPES (pH 7.6), 20 mM KCl, 5 mM $MgCl_2$, 5% glycerol, and 1 mM DTT]. The purity and molecular mass were verified by SDS−PAGE and HPLC electrospray mass spectrometry, confirming the correct primary sequence containing only the N-terminal start methionine.

Human UbcH5a was expressed as a fusion protein with an N-terminal His_{10} tag in bacterial expression strain FI8202/pCodonPlus. The culture was grown to an OD_{600} of 0.8 and induced overnight with 0.5 mM IPTG at 30 °C. Cells were lysed with a French press in buffer C [50 mM Tris-HCl (pH 8.0), 50 mM imidazole, 500 mM KCl, 5 mM $MgCl_2$, and 5% glycerol] containing 1 mM PMSF and DNase. The lysate was clarified by centrifugation (19000 rpm for 60 min), and the supernatant was incubated with Ni-NTA agarose (QIAGEN) for 30 min at 4 °C. The beads were extensively washed with buffer C, and the protein was eluted with elution buffer (buffer C containing 500 mM imidazole). The protein fraction was supplemented with tobacco etch virus (TEV) protease and dialyzed against buffer C overnight. The dialyzed protein was passed over Ni-NTA agarose to remove TEV protease and the His_{10} tag, and flow-through fractions were further purified by anion exchange chromatography.

Circular Dichroism Spectroscopy. Far-UV CD spectra were recorded between 190 and 250 nm with a Jasco J-715 spectropolarimeter. The measurements were performed in 10 mM potassium phosphate (pH 7.4) at a CHIP concentration of 5 μM in the presence or absence of 100 μM synthetic Hsp70 peptide or Hsp90 peptide in a 1 mm cuvette at 30 °C.

Surface Plasmon Resonance Spectroscopy (*SPR*). Sulfhydryl groups of CHIP were biotinylated using biotin-maleimide (Pierce) which was termed bio-CHIP. Monoclonal α-biotin

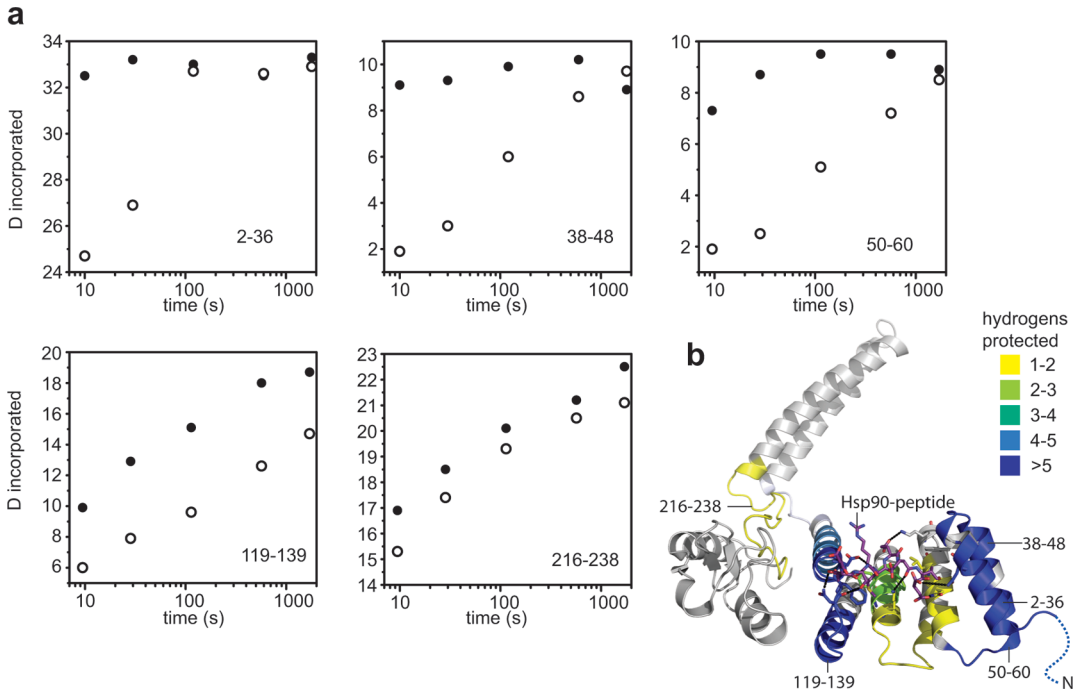

FIGURE 4: Stabilization of CHIP segments upon chaperone binding. (a) Deuteration kinetics of selected CHIP segments as indicated in the apo state (●) and in the presence of hHsc70 (○). (b) Secondary structure representation of the mouse CHIP monomer colored according to the number of amide hydrogens protected upon ligand binding after 30 s in D_2O. Unaffected regions are colored gray.

antibody was immobilized by EDC/NHS coupling on a CM5 sensor chip in a Biacore 3000 instrument. Bio-CHIP was loaded on the antibody-coated cell to 450 resonance units, and increasing concentrations of UbcH5a (0.16−20 μM) diluted in HBS buffer [10 mM HEPES-KOH (pH 7.4), 150 mM NaCl, 5 mM $MgCl_2$, 50 μM EDTA, and 0.005% surfactant P20] were passed over the sensor chip. Unspecific signals from a flow cell coated with the antibody only were subtracted. SPR data were collected at a sampling rate of 1 Hz. Sensorgrams were analyzed using a global fitting model from BIAevaluation version 4.0.1. For the analysis of the CHIP−Hsc70 interaction, a single-cysteine variant of Hsc70 [Hsc70-T111C/C276A/C574A/C603S which is completely functional in vitro (M. Stankiewicz and M. P. Mayer, unpublished results)] was biotinylated using biotin-maleimide and immobilized on a SA sensor chip to 800 resonance units. CHIP (250 nM) and Ubc13 (10−40 μM) in HBS buffer were passed over the sensor chip.

Hydrogen Exchange Experiments and Data Analysis. Hydrogen exchange experiments were performed as described previously (*13*) using an HPLC−MS setup including a column with immobilized pepsin. Peptic peptides of CHIP were identified by MS/MS or by exact mass.

For analysis of complexes, 20 μM ligand free human CHIP was preincubated with 100 μM hHsp70, hHsc70, or hHsp90β for 30 min at 30 °C. For the formation of a complex with octapeptides, 40 μM CHIP was preincubated with 600 μM Hsp90 peptide (ASRMEEVD) or Hsp70 peptide (GPTIEEVD) for 30 min at 30 °C. For the formation of a complex with E2 enzymes, 20 μM CHIP was preincubated with 100 μM Ubc13 or 100 μM UbcH5a for 60 min at 30 °C.

HX was initiated by 20-fold dilution into D_2O buffer [25 mM HEPES (pD 7.4), 50 mM KCl, and 5 mM $MgCl_2$] at 30 °C. After various time intervals, the exchange reaction was stopped by addition of 1 volume of ice-cold quench buffer [0.4 M $K_xH_yPO_4$ (pH 2.2)]. Quenched samples were immediately injected into the HPLC setup, subjected online to pepsin digestion, and analyzed via an ESI-QTOF mass spectrometer (QSTAR Pulsar, Applied Biosystems) as described previously. A fully deuterated CHIP sample was analyzed under the same conditions to correct for back-exchange. Data processing was performed using the method described in ref *13*.

RESULTS

Unliganded CHIP Is a Symmetric Dimer in Solution with Highly Flexible Regions. To analyze the conformational flexibility of human CHIP in solution, we performed HX-MS experiments as described previously (*13*). Briefly, CHIP was diluted 1:20 into D_2O buffer and incubated for different time intervals at 30 °C. The HX reaction was quenched by lowering the temperature to 0 °C and the pH to 2.5, and the samples were injected into our HPLC−MS setup that included a column with immobilized pepsin to generate peptic peptides. The sequence coverage of identified CHIP peptic peptides was 95%, allowing detection of the incorporation of deuterons in all regions of the entire 35 kDa protein (Figure 1b).

HX experiments with unliganded human CHIP revealed highly flexible and dynamic regions in the protein. In particular, the very N-terminal segments of the TPR domain, including residues 2−48[2] and 50−60 (forming the first TP repeat in the crystal structure), seem to be largely unfolded, exchanging 99 and 73% of the accessible amide protons within 10 s in D_2O, respectively (Figures 2a and 4a). The hydrogen exchange behavior of the TPR for apo-CHIP is consistent with a recent NMR

[2]When analyzed peptides are mentioned, the actual residue numbers are given. When exchanged amide protons are mentioned, the first residue of the analyzed peptide is omitted because a peptide of *n* residues has only $n - 1$ amide hydrogens. The amide group of the first residue is converted back to an amino group through proteolytic cleavage and rapidly exchanges back any incorporated deuterons to protons during the desalting step.

study of consensus TPR proteins, which showed that central TPR repeats are more protected from hydrogen exchange than the helix−turn−helix repeats at both ends (Figure 2b) (*14*). After incubation in D_2O for 2 and 30 min, almost all TPR domain peptides completely exchanged their amide protons (Figures 2 and 4a), suggesting a highly dynamic conformation in the helical repeat domain. The solvent accessibility of other regions is in good agreement with crystallographic data, as can be seen in the amide proton protection of helical parts within the hCHIP middle domain (residues 163−168) and the C-terminal U-box domain (Figure 2a) and rapidly exchanging loop regions. The data also monitor the dimeric contacts in CHIP. Both segments in the helical middle domain, residues 163−168 and residues 200−211, exhibit a stable protection even after long exchange time intervals (Figure 2a), consistent with the reported dimer interface of the CHIP crystal structure (*6*). Similarly, the second important hydrophobic dimerization interface in the U-box domain, which is located around Asn^{284} (residues 287−293), is also highly protected from deuterium exchange.

Interestingly, the region including residues 153−161, which is the base of the helical hairpin of the charged middle domain, exchanged almost completely within 10 s (Figure 2a,b and Figure 1 of the Supporting Information). This indicates that hydrogen bonds in this part are not stable in solution. In contrast to expectations from the asymmetric crystal structure of mouse CHIP, no bimodal distribution could be observed in the spectrum of the deuterated peptide, suggesting CHIP is a symmetric dimer in solution with flexible regions in the helical coiled-coil domain. Since the crystal structure of *D. rerio* CHIP lacking the TPR domains shows the protein as a symmetric dimer with the helical hairpin of the middle domain completely folded (Figure 1 of the Supporting Information), we asked whether deletion of the TPR domain in hCHIP would also result in stabilization of this unfolded part into an elongated helix. Deuteron incorporation after HX for 30 s into segment 153−161 of the ΔTPR construct [hCHIP(128−303)] was the same as in the full-length hCHIP (Figure 2c), showing the unchanged high flexibility in this part. However, deletion of the TPR domain led to a slightly increased level of protection of amide hydrogens in segments of the distal part of the middle domain and the U-box region [residues 170−198 and 200−211 (Figure 2c)], demonstrating a destabilizing effect of the unliganded TPR domain on other regions of the full-length protein.

Chaperone Binding Results in Strong Stabilization of the Whole CHIP TPR Domain. CHIP has been shown to bind to the C-terminus of Hsp70 and Hsp90 chaperones with high affinity via its TPR domain (*6*). To analyze possible conformational changes in CHIP induced by individual chaperone binding, we performed HX in the absence and presence of purified Hsp70, Hsc70, and Hsp90 chaperones and their respective eight-residue C-terminal peptides (Figure 3 and data not shown). CHIP was preincubated for 30 min with an excess of full-length chaperone or peptide to allow the formation of a stable complex. After incubation in D_2O for 30 s, the samples were analyzed in our HPLC−MS system, including columns with immobilized pepsin. With the HPLC gradient used in this study, it was possible to separate almost all deuterated CHIP peptides from the majority of chaperone-derived peptides for a detailed analysis of hydrogen exchange. Overall, binding of Hsp70, Hsp90, and their respective C-terminal peptides led to a strong stabilization of the conformation in many parts of the TPR domain of CHIP, as assessed by significant protection from hydrogen exchange in the complex (Figures 3 and 4). Especially the flexible N-terminus with the first helix−turn−helix repeat (segments 2−36, 38−48, and 50−60), the third distal repeat (segment 119−139), and the terminal helix (segment 141−151) of the TPR domain show a strong stabilization in the presence of peptides and full-length chaperones, having a total of ∼35 amide hydrogens protected in the complex compared to the apo form after deuteration for 30 s (Figures 3 and 4a). The adjacent flexible segment, 153−161, exchanged in the presence and absence of chaperones to the same high extent, suggesting no influence of chaperone or peptide binding on the structure of this CHIP region or the symmetry of the protein.

Outside the TPR domain, only a slight protection in the U-box is observed [segment 216−238 (Figure 3)], which may be due to direct contacts between R141 and E239 and between P137 and F238 as suggested by the crystal structure (*6*). No other critical differences in deuteron incorporation were measured between CHIP−chaperone and CHIP−peptide complexes of both the Hsp90 and Hsp70 type. This indicates that there is no additional contribution of full-length chaperone binding to the conformation of CHIP, which is also reflected in similar binding affinities of CHIP for peptide and intact chaperones as measured by ITC (*6*).

To additionally confirm the evident secondary structure stabilization of apo-CHIP in solution by chaperone binding, we conducted circular dichroism spectroscopy with CHIP in the absence or presence of the Hsp70 and Hsp90 octapeptides (Figure 5). Strikingly, the formation of a complex of CHIP with the peptides led to a significant increase in the level of α-helical structure as seen by intensifying bands at 208 and 222 nm as compared to the sum of the spectra of CHIP and the respective peptide separately.

Effects of E2 Enzyme Binding on the Conformation of Full-Length CHIP. We next investigated the influence of binding of different E2 enzymes on the conformational dynamics of full-length CHIP. We therefore purified recombinant human UbcH5a and human Ubc13 which both have been reported to interact with the U-box of CHIP (*6*, *7*). For the interaction of Ubc13 with CHIP, K_d values of 1.3 and 2.8 μM were reported (*6*). We characterized the stable interaction of human UbcH5a with CHIP by SPR and determined a K_d of 2.6 μM (Figure 6a).

We then performed HX experiments with preformed CHIP−UbcH5a and CHIP−Ubc13 complexes with a large excess of the respective E2 enzyme present to ensure a high occupancy of CHIP. When analyzing the HX behavior of the CHIP-derived peptides from a CHIP−UbcH5a complex, we detected subtle effects on the solvent accessibility of the corresponding segments caused by the E2 binding. Upon formation of the complex, a segment in the U-box domain (residues 239−259) and two segments at the distal end of the helical middle domain (including residues 170−211) exhibit protection factors of 0.7, 1.9, and 2.2 amide hydrogens, respectively (Figure 7, cyan and blue segments). The stabilized region of the U-box contains residues (I235 and F237) implicated from the cocrystal structure in the interaction with UbcH5a (*7*) (PDB entry 2OXQ). For the stabilized part at the tip of the middle domain, no explanation is immediately obvious. Interestingly, some segments in the middle and TPR domain exhibited a slight increase in the level of deuteron incorporation upon UbcH5a binding.

In the CHIP−Ubc13 complex, there is also less exchange detected in the segments of the U-box, indicating small conformational changes due to hydrophobic contacts between Ubc13 and this region as shown in the crystal structure (*6*). In

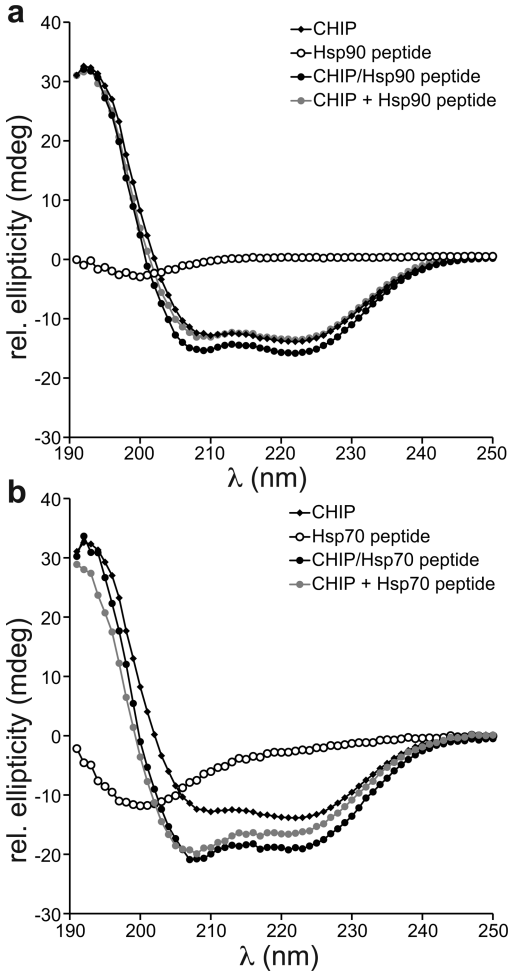

FIGURE 5: Secondary structure formation in hCHIP upon EEVD peptide binding assessed by circular dichroism spectroscopy. (a) CD spectra of apo-hCHIP (◆), Hsp90 EEVD peptide (○), hCHIP in complex with excess Hsp90 peptide (●), and the arithmetic sum of the spectra of apo-hCHIP and the Hsp90 EEVD peptide (gray circles) showing an increased level of formation of α-helical structure. (b) Same as panel a with the Hsp70 EEVD peptide.

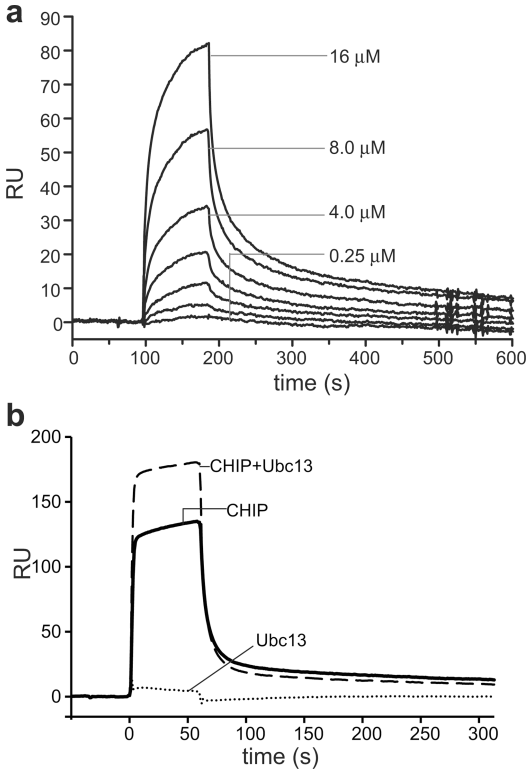

FIGURE 6: Interaction of hCHIP with human UbcH5a and Hsc70 in the presence of Ubc13. (a) SPR sensorgram showing the binding of UbcH5a to biotinylated CHIP on an α-biotin antibody-coated sensor chip. Different concentrations of UbcH5a are indicated. (b) SPR sensorgram showing the binding of hCHIP to biotinylated human Hsc70 immobilized on a SA sensor chip in the absence and presence of Ubc13 as indicated.

contrast to binding of UbcH5a, however, a more prominent deprotection of amide protons could be observed in several segments of the TPR domain (Figure 7a,b, red segments). This raises the question of whether the effect of Ubc13 on the TPR domain of CHIP affects binding of CHIP to chaperones. To investigate this question, we performed HX-MS in the presence of Hsp70, CHIP, and Ubc13. However, the relevant CHIP peptides could not be separated from the peptides of Hsp70 and Ubc13 since these proteins had to be used in excess to ensure complete binding of CHIP. We repeated the experiments using the C-terminal EEVD motif-containing peptide instead of Hsp70 (Figure 8). The resulting difference plot shows additive effects of both interactions (see segments 50−60, 119−139, 141−151, and 170−198 in Figure 8), indicating that Ubc13 and an EEVD motif-containing ligand could bind to CHIP at the same time. To verify independently that Ubc13 and a chaperone can bind to CHIP at the same time, we analyzed the interaction of CHIP with Hsc70 by surface plasmon resonance spectroscopy. We immobilized biotinylated Hsc70 on a streptavidin sensor chip and injected CHIP in the absence and presence of a large excess of Ubc13 (Figure 6b). Injection of Ubc13 alone did not result in an increase in resonance units, demonstrating that Ubc13 does not interact with Hsp70 in the absence of CHIP. CHIP elicited the expected rapid increase in resonance units, indicating interaction with the immobilized Hsc70. Injecting CHIP in the presence of Ubc13 resulted in a significantly increased signal magnitude indicating that a complex of CHIP with Ubc13 interacts with Hsc70. To the best of our knowledge, this is the first demonstration that CHIP in complex with Ubc13 can interact with a chaperone.

DISCUSSION

In this study, we analyzed the conformational properties of human CHIP in solution. Using HX-MS, we resolved the exchangeability of amide hydrogens for the dimeric 35 kDa protein with almost complete sequence coverage, including the very N-terminus, which is not present in crystal structures. In the absence of interaction partners, CHIP is a highly flexible protein. The N-terminus and the adjacent peptides up to residue 60, forming the first helix−turn−helix motif of the TPR domain, seem to be largely unfolded, exchanging almost all accessible amide protons within 10 s, but all other segments in the TPR domain as well as distinct parts of the middle domain and the U-box are also very dynamic and exchange almost all of their amide protons within 30 min. Interaction of CHIP with molecular chaperones Hsp70 and Hsp90, or their respective EEVD-containing C-terminal peptides, leads to a substantial stabilization of the TPR domain and a slight increase in the level of protection in the beginning of the U-box. Binding of E2 ubiquitin-conjugating enzymes UbcH5a and Ubc13 induced a specific protection of a segment in the U-box but also a deprotection in the TPR domain. Under all the conditions that

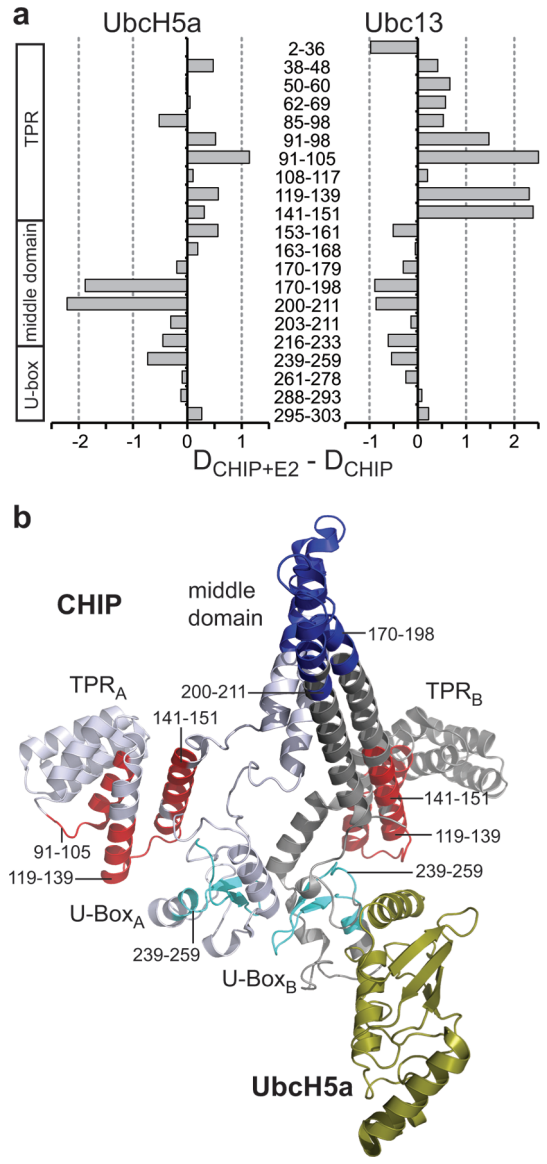

FIGURE 7: Effects of E2 enzyme binding on the CHIP conformation. (a) Differences between incorporation of deuterons into CHIP segments in the presence of E2 enzymes UbcH5a and Ubc13 and incorporation of deuterons into unbound CHIP after deuteration for 30 s. (b) Secondary structure representation of the mouse CHIP dimer (PDB entry 2C2L) with the U-box of one protomer aligned with the U-box of zebrafish CHIP in complex with UbcH5 from the cocrystal structure (PDB entry 2OXQ). Segments stabilized in HX experiments upon UbcH5a binding are colored dark blue (1.9 and 2.2 protons protected) and cyan (0.7 proton protected). Segments colored red are destabilized in the presence of Ubc13.

were tested, the mass spectra of the peptic fragments of CHIP showed a binomial isotope distribution indicating that both CHIP protomers incorporate deuterons to a similar degree. These results argue for a complete equivalence of both protomers in the CHIP dimer and a symmetric conformation.

Our findings appear to be in conflict with two recently published crystal structures of CHIP homologues, one showing a symmetric and the other an asymmetric CHIP dimer (*6*, *8*). The crystal structure of a zebrafish CHIP construct (residues 127−282, corresponding to residues 142−301 in human CHIP) lacking the TPR domains revealed a symmetric dimer with a folded helix in the N-terminal part of the middle domain (helix α7 in the full-length protein) (*8*). In our HX-MS data, the N-terminal part of the middle domain is highly flexible, exchanging almost all amide hydrogens within 10 s suggesting a rather unfolded conformation (Figure 1 of the Supporting Information). The discrepancy between this crystal structure and our data is not likely to be due to the absence of the TPR domains in the crystallized dimer assembly of zebrafish CHIP since a CHIP construct with the TPR domain truncated incorporated deuterons into the beginning of the middle domain to a similar degree.

The crystal structure of mouse CHIP (residues 24−304, corresponding to residues 23−303 in human CHIP) in complex with a C-terminal Hsp90 peptide revealed CHIP to be an asymmetric homodimer, forming one protomer with helix α7 extending into the middle domain and the other protomer forming a "broken" helix α7. If this were the case for human CHIP in solution, a bimodal distribution of the isotope peaks should be observed for the deuterated peptide (residues 152−161) covering this region. A bimodal isotope distribution is indicative for two different coexisting conformational states, with one state being more protected from HX than the other state (*15*). Our HX-MS data revealed that peptide 152−161 is highly flexible without a bimodal distribution of the isotope peaks and thus support a model of a symmetric homodimer that contains a broken helix 7 in both protomers. Because of the high flexibility of this segment, it is possible that this region in the middle domain is rapidly alternating between the helical state and the unfolded state, such that both protomers alternate in turns between the conformation with the broken and the conformation with the continuous helix 7. Since in our HX-MS experiments the shortest incubation time in D_2O was 10 s, any interconversion between two asymmetric states that occurs on a shorter time scale would remain hidden to this method. In the crystals of mouse CHIP, one of the two alternating conformations would then be trapped. In this way, CHIP would be asymmetric at any given moment but symmetric on a time average. However, under physiological conditions, in solution the asymmetric situation of the dimer does not seem to be stabilized even in the presence of ligands. Although the protection in the U-box observed in the presence of the E2 enzymes is too small to exclude a bimodal distribution with certainty, protection (segments 170−198 and 200−211 in the presence of UbcH5a) and deprotection (segments 91−105, 119−139, and 141−151 in the presence of Ubc13) in other parts of CHIP are sufficiently large to allow the detection of a possible bimodal distribution. This calls into question the suggested role of CHIP's asymmetric assembly in connecting the "dimeric" chaperone binding function to the monomeric E2 ubiquitin-conjugating function (*6*).

Our data, showing that the TPR domain is rather loosely folded in the absence of ligand, may explain the aggregation propensity of wild-type CHIP at elevated temperatures, which is diminished in TPR deletion constructs (*16*). The highly dynamic character of CHIP's TPR domain might also contribute to the recently discovered chaperone activity of CHIP. CHIP was shown to possess intrinsic chaperone activity that enables refolding of denatured luciferase and is enhanced under heat stress (*16*). This study suggests that the chaperone activity resides in the TPR domain because CHIP with a deletion of the TPR domain is unable to refold luciferase. It is tempting to speculate that the flexible and unfolded regions in the TPR of ligand-free CHIP expose hydrophobic patches that interact with non-native polypeptides. The highly flexible TPR domain may also interact with native proteins that are ubiquitinated in a CHIP-dependent way in the absence of chaperones (*17*, *18*).

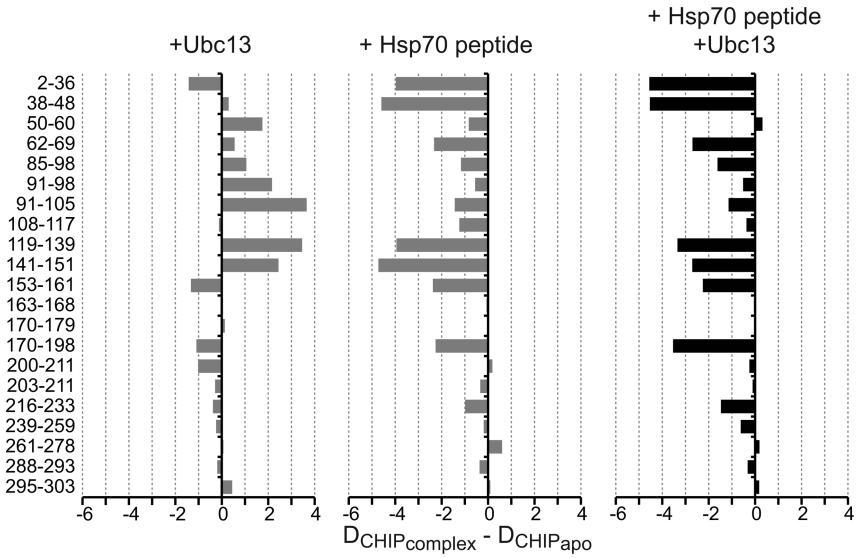

FIGURE 8: Effects of simultaneous binding of Ubc13 and an EEVD motif peptide to CHIP. Differences between incorporation of deuterons into CHIP segments in the presence of Ubc13, octapeptide GPTIEEVD (Hsp70 C-terminus), or both together and incorporation of deuterons into unbound CHIP after deuteration for 30 s.

In addition, the highly solvent exposed N-terminal region of CHIP's TPR domain seems to be an important recognition site for posttranslational modifications. Several proteomic studies report two phosphorylation sites at Ser^{19} and Ser^{23} (*19*−*21*) and a ubiquitination site at Lys^{22} that was identified as autoubiquitination by a GST−CHIP fusion construct in the presence of the E2 enzyme UbcH5a (*22*). The flexibility and accessibility of this region might therefore have an important function for the regulation and specificity of CHIP action.

Our data demonstrate that the dynamics of CHIP's TPR domain is greatly reduced in the presence of Hsp70 and Hsp90 chaperones. Ligand binding induced a significant protection of amide hydrogens, which was most prominent in both repeats flanking the ligand-binding site. This observation is consistent with polar and hydrophobic contacts between the cocrystallized peptide and these parts of the TPR domain (Figure 4b). The stabilization of the helical fold in the TPR domain by ligand binding was also observed in NMR and CD spectroscopic studies of protein phosphatase 5 (PP5) that is targeted to Hsp90 via its N-terminal TPR domain (*23*, *24*). The isolated apo-TPR of PP5 was found to be not fully folded and could be stabilized significantly by addition of the pentapeptide MEEVD, increasing the helical content from 64 to 98% as measured by CD spectroscopy (*23*). The increase in helical content observed in CD experiments described here is not as large, most likely because we analyzed the TPR domain of CHIP in the context of the full-length protein. The TPR domain contains ~50% of the total number of residues in helices as determined from the crystal structure (PDB entry 2C2L). Therefore, a relative change in helical content induced by a ligand binding to the TPR domain would appear to be smaller since it affects only the helices in the TPR domain. In addition, the middle domain and U-box may stabilize the TPR domain, causing a higher degree of helicity in the absence of ligand as compared to an isolated TPR domain. Consistent with such a view are our HX-MS experiments showing that helices 1 and 2 of the TPR domain, which are farthest from the U-box, exchange 80−100% of their amide hydrogens within the dead time of the experiment, while the TPR domain helices adjacent to the U-box exchange only 40−60%. Nevertheless, the helices in the ligand-free TPR domain of CHIP are highly dynamic as shown by our HX-MS experiments. Cliff et al. (*23*) proposed that folding coupled to binding might be a common mechanism of ligand recognition by TPR domains, although this idea has been debated (*14*). However, recently published data on the interaction of the TPR protein Ssn6 with Tup1 emphasize the coupled folding−binding mechanism as a common principle in TPR-mediated interactions (*25*). Our HX-MS data clearly demonstrate that CHIP follows such a folding−binding mechanism as shown in PP5. However, the regions stabilized include mainly outer TPR repeats 1 and 3 of the concave binding surface of CHIP's TPR domain, an effect that is different in PP5 (*24*).

Using HX-MS, we characterized the effect of binding of E2 ubiquitin-conjugating enzymes on CHIP's conformational flexibility. Formation of a complex with both E2 enzymes, canonical UbcH5a and noncanonical Ubc13, both of which bind with micromolar affinity, led to a weak stabilization of U-box peptide 239−259, which contains residues implicated in the interaction in the cocrystal structures of mouse CHIP−U-box−Ubc13 and zebrafish CHIP−U-box−UbcH5 complexes (*6*, *7*). It was proposed that the common E2−E3 interface consists of a hydrophobic ridge of the E2 enzyme bound in a hydrophobic groove between short helix α9 (residues 255−266) and the tips of two hairpin turns (residues 235−240 and 270−274) of the CHIP U-box. The interaction is mainly based on hydrophobic and polar contacts of side chains in which no amide hydrogens of CHIP are involved, explaining the weak protection in hydrogen exchange in the complex. Surprisingly, UbcH5a and Ubc13 affected the dynamics of CHIP in distinct manners. While binding of the canonical UbcH5a had an only small effect on the incorporation of deuterons into the TPR domain, formation of a complex with Ubc13 led to a clear destabilization of numerous segments at the C-terminal end of the TPR domain. These observations point to differences between CHIP's interaction with UbcH5a and Ubc13 and seem to be at odds with the crystal structure of Ubc13 in complex with the U-box of mouse CHIP and UbcH5a in complex with the U-box of zebrafish CHIP (*6*, *7*). Interestingly, truncated forms of CHIP lacking the TPR domain are as active in polyubiquitination as full-length CHIP when paired with Ubc13 and Uev1a, but far less active with UbcH5a (*26*). Chaperones and

Ubc13 have opposing effects on the TPR domain of CHIP. In particular, helix α7, which is critical for the stability of the whole TPR domain, is affected most upon Ubc13 binding (*27*). Nevertheless, HX experiments using an EEVD peptide indicated that both Ubc13 and the EEVD peptide can bind to CHIP simultaneously. Consistent with these results, a ternary complex of CHIP, Ubc13, and Hsc70 was also observed by SPR. Thus, the opening of parts of the TPR domain by interaction of CHIP with Ubc13 did not negatively affect interaction with chaperones. However, this Ubc13-induced opening may positively influence the interaction of CHIP with other substrates, allowing more modes of interaction in addition to the acidic clamp binding of the C-terminal EEVD motif of Hsp70 and Hsp90 chaperones.

ACKNOWLEDGMENT

We thank T. Ruppert for his support in the mass spectrometry facility of the ZMBH.

SUPPORTING INFORMATION AVAILABLE

A figure depicting the conformational flexibility of CHIP. This material is available free of charge via the Internet at http://pubs.acs.org.

REFERENCES

1. Arndt, V., Rogon, C., and Hohfeld, J. (2007) To be, or not to be: Molecular chaperones in protein degradation. *Cell. Mol. Life Sci. 64*, 2525–2541.
2. Cyr, D. M., Hohfeld, J., and Patterson, C. (2002) Protein quality control: U-box-containing E3 ubiquitin ligases join the fold. *Trends Biochem. Sci. 27*, 368–375.
3. Nikolay, R., Wiederkehr, T., Rist, W., Kramer, G., Mayer, M. P., and Bukau, B. (2004) Dimerization of the human E3 ligase CHIP via a coiled-coil domain is essential for its activity. *J. Biol. Chem. 279*, 2673–2678.
4. Pickart, C. M. (2001) Mechanisms underlying ubiquitination. *Annu. Rev. Biochem. 70*, 503–533.
5. Murata, S., Minami, Y., Minami, M., Chiba, T., and Tanaka, K. (2001) CHIP is a chaperone-dependent E3 ligase that ubiquitylates unfolded protein. *EMBO Rep. 2*, 1133–1138.
6. Zhang, M., Windheim, M., Roe, S. M., Peggie, M., Cohen, P., Prodromou, C., and Pearl, L. H. (2005) Chaperoned ubiquitylation: Crystal structures of the CHIP U box E3 ubiquitin ligase and a CHIP-Ubc13-Uev1a complex. *Mol. Cell 20*, 525–538.
7. Xu, Z., Kohli, E., Devlin, K. I., Bold, M., Nix, J. C., and Misra, S. (2008) Interactions between the quality control ubiquitin ligase CHIP and ubiquitin conjugating enzymes. *BMC Struct. Biol. 8*, 26.
8. Xu, Z., Devlin, K. I., Ford, M. G., Nix, J. C., Qin, J., and Misra, S. (2006) Structure and interactions of the helical and U-box domains of CHIP, the C terminus of HSP70 interacting protein. *Biochemistry 45*, 4749–4759.
9. Busenlehner, L. S., and Armstrong, R. N. (2005) Insights into enzyme structure and dynamics elucidated by amide H/D exchange mass spectrometry. *Arch. Biochem. Biophys. 433*, 34–46.
10. Hoofnagle, A. N., Resing, K. A., and Ahn, N. G. (2003) Protein analysis by hydrogen exchange mass spectrometry. *Annu. Rev. Biophys. Biomol. Struct. 32*, 1–25.
11. Wales, T. E., and Engen, J. R. (2006) Hydrogen exchange mass spectrometry for the analysis of protein dynamics. *Mass Spectrom. Rev. 25*, 158–170.
12. Andreasson, C., Fiaux, J., Rampelt, H., Mayer, M. P., and Bukau, B. (2008) Hsp110 is a nucleotide-activated exchange factor for Hsp70. *J. Biol. Chem. 283*, 8877–8884.
13. Rist, W., Graf, C., Bukau, B., and Mayer, M. P. (2006) Amide hydrogen exchange reveals conformational changes in hsp70 chaperones important for allosteric regulation. *J. Biol. Chem. 281*, 16493–16501.
14. Cortajarena, A. L., and Regan, L. (2006) Ligand binding by TPR domains. *Protein Sci. 15*, 1193–1198.
15. Wales, T. E., and Engen, J. R. (2006) Partial unfolding of diverse SH3 domains on a wide timescale. *J. Mol. Biol. 357*, 1592–1604.
16. Rosser, M. F., Washburn, E., Muchowski, P. J., Patterson, C., and Cyr, D. M. (2007) Chaperone functions of the E3 ubiquitin ligase CHIP. *J. Biol. Chem. 282*, 22267–22277.
17. Li, R. F., Zhang, F., Lu, Y. J., and Sui, S. F. (2005) Specific interaction between Smad1 and CHIP: A surface plasmon resonance study. *Colloids Surf., B 40*, 133–136.
18. Xin, H., Xu, X., Li, L., Ning, H., Rong, Y., Shang, Y., Wang, Y., Fu, X. Y., and Chang, Z. (2005) CHIP controls the sensitivity of transforming growth factor-β signaling by modulating the basal level of Smad3 through ubiquitin-mediated degradation. *J. Biol. Chem. 280*, 20842–20850.
19. Imami, K., Sugiyama, N., Kyono, Y., Tomita, M., and Ishihama, Y. (2008) Automated phosphoproteome analysis for cultured cancer cells by two-dimensional nanoLC-MS using a calcined titania/C18 biphasic column. *Anal. Sci. 24*, 161–166.
20. Beausoleil, S. A., Villen, J., Gerber, S. A., Rush, J., and Gygi, S. P. (2006) A probability-based approach for high-throughput protein phosphorylation analysis and site localization. *Nat. Biotechnol. 24*, 1285–1292.
21. Olsen, J. V., Blagoev, B., Gnad, F., Macek, B., Kumar, C., Mortensen, P., and Mann, M. (2006) Global, in vivo, and site-specific phosphorylation dynamics in signaling networks. *Cell 127*, 635–648.
22. Wang, D., Xu, W., McGrath, S. C., Patterson, C., Neckers, L., and Cotter, R. J. (2005) Direct identification of ubiquitination sites on ubiquitin-conjugated CHIP using MALDI mass spectrometry. *J. Proteome Res. 4*, 1554–1560.
23. Cliff, M. J., Williams, M. A., Brooke-Smith, J., Barford, D., and Ladbury, J. E. (2005) Molecular recognition via coupled folding and binding in a TPR domain. *J. Mol. Biol. 346*, 717–732.
24. Cliff, M. J., Harris, R., Barford, D., Ladbury, J. E., and Williams, M. A. (2006) Conformational diversity in the TPR domain-mediated interaction of protein phosphatase 5 with Hsp90. *Structure 14*, 415–426.
25. Palaiomylitou, M., Tartas, A., Vlachakis, D., Tzamarias, D., and Vlassi, M. (2008) Investigating the structural stability of the Tup1-interaction domain of Ssn6: Evidence for a conformational change on the complex. *Proteins 70*, 72–82.
26. Windheim, M., Peggie, M., and Cohen, P. (2008) Two different classes of E2 ubiquitin-conjugating enzymes are required for the mono-ubiquitination of proteins and elongation by polyubiquitin chains with a specific topology. *Biochem. J. 409*, 723–729.
27. Main, E. R., Xiong, Y., Cocco, M. J., D'Andrea, L., and Regan, L. (2003) Design of stable α-helical arrays from an idealized TPR motif. *Structure 11*, 497–508.